AAC Accepted Manuscript Posted Online 24 June 2019
Antimicrob. Agents Chemother. doi:10.1128/AAC.00207-19

Rapid evolution of reduced susceptibility against a balanced dual-targeting antibiotic through stepping-stone mutations

Petra Szili[1,6§], Gábor Draskovits[1§], Tamás Révész[1,5§], Ferenc Bogar[2,3], Dávid Balogh[1], Tamás Martinek[3], Lejla Daruka[1], Réka Spohn[1], Bálint Márk Vásárhelyi[1], Márton Czikkely[1,7], Bálint Kintses[1,8], Gábor Grézal[1], Györgyi Ferenc[4], Csaba Pál*[1], Ákos Nyerges*[1]

[1]Synthetic and Systems Biology Unit, Institute of Biochemistry, Biological Research Centre of the Hungarian Academy of Sciences, Szeged, Hungary;
[2]MTA-SZTE Biomimetic Systems Research Group, University of Szeged, Szeged, Hungary;
[3]Department of Medical Chemistry, University of Szeged, Szeged, Hungary;
[4]Nucleic Acid Synthesis Laboratory, Biological Research Centre of the Hungarian Academy of Sciences, Szeged, Hungary;
[5]Doctoral School of Theoretical Medicine, University of Szeged, Szeged, Hungary;
[6]Doctoral School of Multidisciplinary Medical Sciences, University of Szeged, Szeged, Hungary;
[7]Szeged Scientists Academy, Szeged, Hungary
[8]Department of Biochemistry and Molecular Biology, University of Szeged, 6726 Szeged, Közép fasor 52, Hungary

[§]These authors have contributed equally to this work.

*To whom correspondence should be addressed: Email: nyerges.akos@brc.mta.hu or pal.csaba@brc.mta.hu.

Abstract

Multi-targeting antibiotics, i.e., single compounds capable of inhibiting two or more bacterial targets are generally considered as a promising therapeutic strategy against resistance evolution. The rationale for this theory is that multi-targeting antibiotics demand the simultaneous acquisition of multiple mutations at their respective target genes to achieve significant resistance. The theory presumes that individual mutations provide little or no benefit to the bacterial host. Here we propose that such individual, stepping-stone mutations can be prevalent in clinical bacterial isolates, as they provide significant resistance to other antimicrobial agents. To test this possibility, we focused on gepotidacin, an antibiotic candidate that selectively inhibits both bacterial DNA gyrase and topoisomerase IV. In a susceptible organism, *Klebsiella pneumoniae*, a combination of two specific mutations in these target proteins provide an over 2000-fold reduction in susceptibility, while individually none of these mutations affect resistance significantly. Alarmingly, strains with decreased susceptibility against gepotidacin are found to be as virulent as the wild-type *Klebsiella pneumoniae* strain in a murine model. Moreover, numerous pathogenic isolates carry mutations which could promote the evolution of clinically significant reduction of susceptibility against gepotidacin in the future. As might be expected, prolonged exposure to ciprofloxacin, a clinically widely employed gyrase inhibitor, co-selected for reduced susceptibility against gepotidacin. We conclude that extensive antibiotic usage could select for mutations that serve as stepping-stones towards resistance against antimicrobial compounds still under development. Our research indicates that even balanced multi-targeting antibiotics are prone to resistance evolution.

Introduction

Antibiotic discovery has been driven by the need for new therapeutics that are not subject to rapid resistance development. Due to the rise of drug-resistant bacteria, the commercial success of antibiotic development is unpredictable(1, 2). Antibiotic combination therapy has long been suggested as a potential strategy to delay resistance evolution(3, 4). The rationale for this theory is that drugs with different modes of action generally require different mutations in respective target genes to achieve resistance, and the simultaneous acquisition of multiple specific mutations is exceedingly rare. Although successful in many cases, antimicrobial combination therapy suffers from several limitations(5, 6). Multi-target antibiotic strategy is an emerging alternative. There are multiple mechanisms by which antimicrobial compounds may inhibit multiple bacterial targets. In the case of hybrid drugs, two antibiotic pharmacophores with dissimilar targets are covalently linked to form one molecule. Other antibiotic compounds equipotently target two or more homologous proteins. Indeed, resistance to linezolid has typically been associated with multiple mutations in varying numbers of copies of the genes encoding 23S ribosomal RNA, all of which have limited effects on resistance individually (7). Finally, they may target multiple, non-overlapping regions of a single bacterial protein. Currently, designing multi-target antibiotics is a major focus of the pharmaceutical industry, but until now relatively few drugs have been demonstrated to achieve a balanced inhibition of multiple microbial targets. (8–10) Due to the shortage of in-depth resistance studies, our knowledge on the tempo and mode of resistance development against multi-target antibiotics remains limited (but see(11–13)).

Gepotidacin (GSK2140944) is an exemplary candidate to study resistance evolution towards multi-targeting antibiotics (Figure 1A). Gepotidacin is a novel triazaacenaphthylene antibiotic candidate currently in phase 2b clinical trials(14, 15) and is expected to enter the clinical practice in the upcoming years(16, 17). The molecule inhibits bacterial DNA gyrase and topoisomerase IV with a novel mode of action. Using a standard frequency-of-resistance test recent studies have failed to identify resistant clones of *Neisseria gonorrhoeae* and *Escherichia coli* against this new compound(8, 18), suggesting that individual mutations cannot provide substantial resistance to gepotidacin. It is especially active against Gram-negative pathogens, such as *Klebsiella pneumoniae*. According to the WHO, infections caused by multi-drug resistant *Klebsiella* strains are emerging as a top-ranked challenge in the health-care sector(19). In this work, we demonstrate that contrary to expectations,

reduced susceptibility to gepotidacin evolves rapidly in *K. pneumoniae,* which has potential implications for the future clinical use of this new antibiotic candidate.

Results

Molecular modelling with directed evolution accurately predicts the positions and impact of resistance mutations

Prior studies have demonstrated that gepotidacin selectively inhibits both bacterial DNA gyrase and topoisomerase IV by a unique mechanism(8, 16), but the exact molecular mechanisms of inhibition have not been thoroughly characterized. Therefore, we first sought to study the exact molecular interactions between gepotidacin and *Escherichia coli*'s DNA gyrase and topoisomerase IV protein complexes, using molecular modelling (Materials and Methods and Supplementary Note 1). Molecular dynamics simulations capture the atomic interactions between the drug and the target protein in time (Supplementary Figure S1). The analysis has revealed that D82 in the GyrA subunit of DNA gyrase and the homologous position, D79 of the ParC subunit of topoisomerase IV form an intermolecular salt bridge with gepotidacin (Figure 1B and C, Supplementary Note 2, and Supplementary Figure S1 and S2). Therefore, mutations at these binding sites are expected to provide reduced susceptibility to gepotidacin, and it was indeed so (see below).

Previously we subjected the potential target genes to a single round of DIvERGE mutagenesis in *E. coli,* and next subjected the mutant library to gepotidacin stress, followed by sequencing the isolates with reduced susceptibility (18). As gepotidacin has not entered clinical use and thus, its clinical breakpoint is not established, we defined reduced susceptibility to gepotidacin as the MIC value that is equal or higher than the peak plasma concentration of the drug (9 μg/ml, (14)). In our current work, the analysis has been repeated in *K. pneumoniae* using nearly identical experimental settings (Figure 1D). The results of the mutagenesis assays are qualitatively the same for the two species: D82 within the GyrA subunit and D79 of the ParC subunit are found to be mutated in all the clones isolated, and no further mutations have been found (Supplementary Table S4). Moreover, subsequent saturation mutagenesis of the two mutational hot-spots has recapitulated that

the combination of these two specific mutations (GyrA D82N, ParC D79N) is responsible for a high-level of reduced susceptibility to gepotidacin (Supplementary Table S4).

To understand the molecular mechanisms behind the reduced susceptibility, we have computationally modelled the molecular interactions between gepotidacin and asparagine mutants at GyrA D82 and ParC D79 positions using molecular dynamics simulations and the Molecular Mechanics/Generalized Born Surface Area (MM-GBSA)(20) method. MM-GBSA has predicted that the observed mutations (GyrA D82N and ParC D79N) weaken the interaction between the target proteins and gepotidacin. (Supplementary Figure S1.). Thus, the combination of DIvERGE mutagenesis assays and molecular dynamics simulations have revealed the putative binding sites for gepotidacin in DNA gyrase and topoisomerase IV protein complexes. Furthermore, the disruption of an indispensable salt bridge between the drug and its two binding sites resulted in high-level reduction of susceptibility in *K. pneumoniae*.

Exceptionally strong synergism between mutations associated with reduced susceptibility

Next, we have studied the individual, as well as the combined effects of these mutations on susceptibility. For this purpose, the mutations were inserted individually into the genomes of *E. coli* K-12 MG1655 and *K. pneumoniae* ATCC 10031. The double-mutants were found to display an over 560- and a 2080-fold reduction in gepotidacin susceptibility level compared to the corresponding wild-type strains of *E. coli* and *K. pneumoniae,* respectively (Table 1, see also ref (21)). In contrast, the single-mutants were found to show no considerable changes in gepotidacin susceptibility in both species (Table 1). These findings are consistent with prior single-step resistance selection studies that failed to recover mutants with significant resistance(8, 18).

Fitness cost of decreased gepotidacin susceptibility is limited

Antibiotic resistance typically induces a fitness cost in the form of reduced bacterial growth rates(22), and such costs shape the long-term stability of antibiotic-resistant populations(23–25). Thus, we have investigated the fitness effects of target-mediated reduction of susceptibility to gepotidacin in *K. pneumoniae*. For this aim we have studied the wild-type and mutant *K. pneumoniae* strains, the latter carrying mutations associated with reduced susceptibility to gepotidacin or fluoroquinolones.

The fluoroquinolone resistance-causing mutations in point are widespread in clinical isolates(26–28) and affect the same genes (namely, *gyrA* and *parC*), therefore they provide a benchmark to estimate the fitness costs compared to the wild-type strain. Relative fitness was estimated by pairwise competition experiments between the wild-type strain and a specific mutant strain in nutrient-rich, antibiotic-free bacterial medium (MHBII) at 37°C. Using established protocols, we have found that the mutation combination of GyrA D82N and ParC D79N which confers reduced susceptibility to gepotidacin significantly decreases fitness in *K. pneumoniae*. However, the fitness cost of gepotidacin resistance-associated mutations is comparable to the fitness cost of canonical, clinically relevant fluoroquinolone resistance-causing mutations. Importantly, ParC D79N mutation is found to confer no measurable fitness cost individually (Figure 2A). Our findings remained the same when active human blood serum was added to the medium.

Mutants with reduced susceptibility to gepotidacin display no changes in virulence in a murine infection model

We next investigated whether mutants with reduced susceptibility to gepotidacin display reduced virulence *in vivo*. As drug-resistant *K. pneumoniae* is frequently responsible for wound and systemic infections, we have studied a murine thigh wound infection model(29, 30). Specifically, we have examined the wound colonization capacity of the wild-type strain, as well as that of representative *K. pneumoniae* mutants with reduced gepotidacin or ciprofloxacin susceptibility. For this purpose, the wild-type strain, as well as each isogenic mutant strain was inoculated into the thigh tissue of female ICR mice (n = 5). After 26 hours, bacterial colonization was determined by plating thigh tissue homogenates to MHBII agar plates. No significant decrease in *in vivo* virulence was observed for any of the mutants compared to the wild-type strain (Figure 2B). It is worth noting however that performing *in vivo* competition experiments in a mouse infection model would also be desirable to further characterize the *in vivo* virulence of the mutations causing reduced susceptibility to gepotidacin and in future work we plan to analyze that.

Cross-resistance analysis between gepotidacin and ciprofloxacin

Several prior works demonstrate that certain resistance mutations are present in bacterial populations long before being exposed to an antibiotic in point. Thus, we hypothesized that prolonged use of other antibiotics might select for mutations that serve as stepping-stones towards reduced susceptibility to gepotidacin. The best candidate antibiotic family is fluoroquinolones, as they are widely employed in clinical practice, and similarly to gepotidacin, they target the gyrase/topoisomerase protein complexes, albeit with a notably different molecular mechanism(17, 31). Moreover, the putative binding sites of gepotidacin and fluoroquinolones on the GyrA protein are adjacent to each other, separated by a single amino acid only (see figure 1B, and refs (32–34)). Despite the functional similarities between these drug classes, a prior paper reported that fluoroquinolone-resistant clinical isolates displayed no cross-resistance to gepotidacin(17).To re-investigate this issue, we have focused on ciprofloxacin, a widely employed and well-characterized fluoroquinolone drug. Several ciprofloxacin-resistance conferring mutations and mutation combinations in clinical isolates provide no relevant cross-resistance against gepotidacin (Supplementary Table S5.). More surprising results have emerged by testing the effect of mutations conferring reduced susceptibility to gepotidacin on ciprofloxacin susceptibility. We have found that the GyrA D82N single-mutant strain displays an over 16-fold increase in ciprofloxacin-resistance level compared to the wild-type *K. pneumoniae* ATCC 10031 strain. This finding is even more remarkable if we consider that the same mutation confers only a twofold increase in gepotidacin MIC level. As might be expected, the GyrA D82N and ParC D79N double-mutants also display significant resistance to ciprofloxacin (Table 1).

Our findings raise the possibility that the D82N mutation of GyrA might be present in fluoroquinolone-resistant clinical isolates, rendering the subsequent emergence of double-mutants with reduced susceptibility to gepotidacin feasible. We have systematically investigated the prevalence of the GyrA D82N and ParC D79N mutations in currently available sequence databases (as of 9 October 2018). Systematic sequence search has revealed that both mutations occur in a wide range of Gram-negative and Gram-positive bacteria (Supplementary Table S2 and Supplementary Figure S4, also Supplementary File 1), including fluoroquinolone-resistant clinical isolates of *E. coli*(35), and other species belonging to the *Salmonella,* the *Mycoplasma, Clostridium, Citrobacter, Streptococcus,* and *Neisseria* genera. *Neisseria* and *Streptococcus* are especially noteworthy, as infections caused by these genera are reported to be the targets of gepotidacin in recent clinical

trials(14, 15, 36). These results indicate that several clinically occurring human pathogens require only a single extra mutation to evolve highly reduced susceptibility to gepotidacin.

Ciprofloxacin stress selects for reduced susceptibility to gepotidacin in the laboratory

To establish further that ciprofloxacin promotes reduced susceptibility to gepotidacin, we have initiated laboratory evolution under ciprofloxacin stress with wild-type *K. pneumoniae* ATCC 10031, as well as the wild-type and Δ*mutS* strains of *E. coli* K-12 MG1655. The previously established protocol aims to maximize the level of drug resistance in the evolving populations that develop in a fixed time period,(37–39) being approximately 116 generations in our case. Six parallel evolving populations of each strain were exposed to gradually increasing concentrations of ciprofloxacin. In line with previous clinical and laboratory studies(31, 40), ciprofloxacin resistance was seen to emerge quickly in our experiments (Figure 3A), especially in Δ*mutS* hypermutator lineages. Despite the short time-frame, all *E. coli* and *K. pneumoniae* populations reached ciprofloxacin-resistance levels equal to or above the EUCAST clinical breakpoint(41) (Figure 3A and 3B). Three randomly selected, ciprofloxacin resistant lineages per strain were selected for gepotidacin MIC measurements. Strikingly, all have been found to display an over 64 to 1058-fold decrease in gepotidacin susceptibility level compared to the corresponding control strains (Figure 3B). Next, we carried out of whole genome sequence analysis of 2 and 3 evolved lineages derived from *E. coli* K-12 MG1655 and *K. pneumoniae* ATCC 10031, respectively. Although these lineages display markedly reduced gepotidacin susceptibilities (Figure 3B), they do not carry mutations at GyrA D82 or ParC D79, suggesting that multiple other mutations may also select for reduced susceptibility to gepotidacin. Indeed, the whole genome sequencing has revealed that these ciprofloxacin resistant lineages carry putative resistance mutations in genes involved in membrane efflux (acrR, soxR, marR) and general stress response (cusS, rpoB) (Supplementary Table S3). Overall, these results strongly suggest that long-term exposure to ciprofloxacin stress promotes reduced susceptibility to gepotidacin.

Discussion

In this work, we have primarily focused on studying the evolution of reduced susceptibility to gepotidacin in *Klebsiella pneumoniae.* As gepotidacin shows excellent potency against Gram-negative bacteria(16, 17, 42), it could offer a last resort drug to treat multidrug-resistant *Klebsiella*

infections. However, we have demonstrated that two specific mutations in the genes encoding gepotidacin's targets can provide a drastically reduced susceptibility in multiple enterobacterial species(21) (see also Table 1). These two mutations (GyrA D82N and ParC D79N) overlap with the predicted binding sites of the drug and show extreme synergism. By abolishing indispensable drug-target interactions, they confer an over 2000-fold reduction in susceptibility, but individually they have only limited effects on susceptibility to gepotidacin. Alarmingly, the double-mutant *K. pneumoniae* strain is as virulent as the wild-type in a mouse infection model, suggesting that these mutations might have clinical significance. Indeed, *Neisseria gonorrhoeae* strains with reduced susceptibility to gepotidacin were isolated in a human clinical phase 2b trial carried a ParC D86N mutation(36) that corresponds to the homologous ParC D79N mutation in *E. coli*.

According to what we term the "stepping-stone" hypothesis, prolonged clinical deployment of certain antibiotics may select for variants with an elevated potential to evolve resistance to new antimicrobial agents. For example, in *Staphylococcus aureus* the genetic alteration responsible for methicillin-resistance had emerged due to the selective pressure of first-generation beta-lactams, such as penicillin, years before methicillin was first applied in clinical practice(43). Hierarchical resistance-acquisition is also predominant during the evolution of resistance to fluoroquinolone antibiotics(44, 45). Furthermore, the byproducts of drug degradation were also shown to promote resistance development against clinically applied antibacterials(46).

To investigate the feasibility of the "stepping-stone" hypothesis, here we have focused on ciprofloxacin, a widely employed and well-characterized fluoroquinolone antibiotic(47). Similarly to gepotidacin, mutations in GyrA and ParC contribute to resistance to ciprofloxacin. Strikingly, mutations kinked to reduced susceptibility to gepotidacin (i.e., GyrA D82N, ParC D79N) increase resistance to ciprofloxacin and have been detected in clinical isolates of ciprofloxacin-resistant bacteria, including strains of *N. gonorrhoeae*, *Streptococcus sp.,* and *S. enterica*. Therefore, these isolates are expected to require only one extra mutational step to develop a reduced susceptibility to gepotidacin.

The "stepping-stone" hypothesis may have general implications. For example, zoliflodacin (ETX0914), a novel bacterial topoisomerase inhibitor has just completed a human phase 2 clinical trial(48). It shows promising activity against multidrug-resistant infections, including *N. gonorrhoeae*(49). However, in this species mutations in GyrB have been reported to confer

zoliflodacin-resistance(50), and one of these zoliflodacin-resistant mutants (D429N) has already been detected in clinical populations(51). As the homologous GyrB mutation (D426N) in *E. coli* confers resistance to fluoroquinolones(21), fluoroquinolone agents might have incidentally selected for reduced susceptibility to zoliflodacin as well. Consistent with this hypothesis, naturally occurring zoliflodacin-resistant variants were also found to be highly resistant to fluoroquinolones(51).

In summary, our work demonstrates that despite a balanced *in vivo* targeting of multiple proteins, high-level resistance can rapidly emerge to antibiotics when the drug molecule's inhibitory effect depends merely on interactions with a few, indispensable amino acids. It is an open issue whether this conclusion holds for a drug that inhibits two completely novel targets. Moreover, based on adaptive laboratory evolution and clinical data, we propose that target gene mutations conferring resistance to fluoroquinolones can facilitate resistance evolution to novel topoisomerase-targeting antimicrobials, including gepotidacin. Therefore, existing resistant bacteria could serve as an immediate source of novel resistance mechanisms. As a more general concept, our work indicates that even drugs executing a balanced multi-targeting of bacterial proteins are prone to resistance, and multi-targeting itself does not preclude the appearance of high-level resistance to antimicrobials. Regarding that a quarter of the antibiotics currently under clinical development target bacterial topoisomerases(52), further research is warranted to test this scenario.

Materials and Methods

Media and antibiotics

For general growth of bacteria and electrocompetent cell preparation, Lysogeny-Broth-Lennox (LB), medium was used (10 g tryptone, 5 g yeast extract, 5 g sodium chloride per 1 l of water). For cell recovery after electroporation, we applied Terrific Broth (TB) (24 g yeast extract, 12 g tryptone, 9.4 g K_2HPO_4, and 2 g KH_2PO_4 per 1 l of water). For antimicrobial susceptibility tests and the selection of resistant variants, cation-adjusted Mueller Hinton II Broth (MHBII) was used. To prepare MHBII broth, 22 g of MHBII powder (Becton Dickinson and Co.) was dissolved in 1 l of water (3 g beef extract, 17.5 g acid hydrolysate of casein and 1.5 g starch). MHBII agar was prepared by the addition of 14 g Bacto agar to 1 l bacterial MHBII broth. Bacterial media were sterilized by autoclaving 15 min at 121 °C. To distinguish lacZ knockout strains and wild-type strains, sterile solutions of X-gal (5-bromo-4-chloro-3-indolyl-β-D-galactopyranoside) and IPTG (isopropyl β-D-1-thiogalactopyranoside) were added to the MHBII agar medium after autoclaving. Final X-gal and IPTG concentration in the medium were 40 mg/l and 0.2 µM, respectively. Antibiotics and chemicals were ordered from Sigma-Aldrich (ampicillin, kanamycin, chloramphenicol; X-gal, IPTG), from Fluka Analytical (ciprofloxacin), and MedChemExpress (gepotidacin).

Oligonucleotides

Sequences of all synthetic DNA oligonucleotides (oligos) are listed in Supplementary file 1. Oligonucleotides were synthesized at the Nucleic Acid Synthesis Laboratory of the Biological Research Centre of the Hungarian Academy of Sciences. Soft-randomized DIvERGE oligos were manufactured according to a previously described soft-randomization protocol(21). PCR primers were purified with standard desalting, while mutagenic oligos were purified with high-performance liquid chromatography (HPLC). Lyophilized oligos were dissolved in 1× Tris-EDTA (TE) buffer, pH 8 (Integrated DNA Technologies) at a final concentration of 100 µM. DIvERGE oligos were dissolved in 0.5× TE buffer at a final concentration of 500 µM. Dissolved oligos were stored at -20 °C.

Homology model building

Crystal structure of *Staphylococcus aureus* in complex with compound GSK945237 (PDB code: 5NPP,(1) resolution of 2.22 Å) was chosen as a template to build a homology model of *Escherichia*

coli DNA Gyrase using Prime from the Schrödinger package(2, 3). GSK945237 is also a member of novel bacterial topoisomerase inhibitors (NBTI) therefore its binding position can serve as a template in our study. The homology model of Topoisomerase IV of *Escherichia coli* was created by using the X-ray structure of *Klebsiella pneumoniae* in complex with levofloxacin (PDB code: 5EIX(8)b, resolution of 3.35 Å) as a template. In the case of DNA Gyrase the DNA chain and the ligand GSK945237 (with both binding poses) were directly transferred from the template PDB structure 5NPP. Since the DNA binding of the two enzyme shows high similarity, the DNA chain and the ligand was also transferred from 5NPP to the homology model of Topoisomerase IV after fitting the backbone atoms of the two proteins. In both cases the protein DNA contacts were checked and corrected separately using local conformation search and minimization.

Computational docking of gepotidacin

We docked gepotidacin (ChemSpider ID: 34982930) into the DNA gyrase and topoisomerase IV homology models using Glide from the Schrödinger package(53). The protonation state of gepotidacin was selected as the main species obtained from pKa calculation using the calculator plugin of Marvin program(54). For Glide docking we used OPLS3 force field(55) and the standard precision procedure with flexible ligand geometries and enhanced conformational sampling. Based on the high similarity of the mode-of-action of GSK945237 and gepotidacin(42), we picked the docking pose of gepotidacin that was most similar to the binding pose of GSK945237 in 5NPP structure. This procedure was repeated for the other docking-pose of GSK945237, as well. Finally, the binding site (defined as residues closer than 5 Å to the ligand) geometry together with the docked ligand was optimized. We followed the same steps in the case of both homology models.

Molecular dynamics simulations of gepotidacin bound DNA-gyrase and DNA-topoisomerase IV complexes

To perform molecular dynamics-based binding mode analysis for gepotidacin at both of its targets, we first parametrized the complex of formed by gepotidacin-DNA- and its corresponding target (DNA gyrase and topoisomerase IV, respectively). For parametrization, we used OPLS3 force field(55). Next, this system was solvated using the SPC (simple point charge) explicit water model(56) within an orthorhombic box 10 Å apart. On the course of simulations, NaCl in 0.15 M final concentration was

used to mimic the physiological conditions. 100 ns molecular dynamics calculations were carried out on these systems at constant volume and temperature (NVT) using the Desmond molecular dynamics code[79]. Snapshots of these simulations were used as a conformational ensemble in mutation-induced binding free energy change calculations.

Estimation of mutation-induced binding free energy changes

Asparagine-mutation induced changes of the binding affinity ($\Delta\Delta G_B$) of gepotidacin at GyrA D82, and ParC D79 positions were calculated as the difference of their binding free energy in the mutated and wild-type enzyme ($\Delta\Delta G_B = \Delta G_B^{MUT} - \Delta G_B^{WT}$). This affinity change was estimated by using Residue Scanning module of Bioluminate package(58) and was based on molecular mechanics-generalized Born surface area (MM-GBSA) approximation[21]. Specifically, we estimated the binding free energy of a ligand (ΔG) by using the single trajectory approach(59) in which a single molecular dynamics simulation of the protein-ligand complex is completed first and sample geometries are collected from the trajectory to represent the possible binding conformations. ΔG is calculated for every single geometry as

$$\Delta G = G_{PL} - G_P - G_L,$$

where G_{PL}, G_P and G_L are the energy of the protein ligand complex, protein and ligand, respectively. These energy values are calculated as

$$G = G_{MM} + G_{Solv},$$

where G_{MM} is the calculated molecular mechanics energy for the force field applied, and G_{Solv} is the solvation energy in the generalized Born approximation. Different variations of this method are widely used in large scale drug design studies[81–83] as it accurately predicts mutational effects in drug-protein interaction analyses with a manageable computational demand (see *e.g.* references(63, 64)). In our study, MM-GBSA calculations were carried out with the *thermal_mmgbsa.py* script Schrödinger package(58) from 100, evenly spaced structures from the second 50 ns of our previously performed molecular-dynamics simulation between the wild-type enzyme (DNA gyrase and topoisomerase IV) and gepotidacin.

Plasmid construction

To perform ssDNA recombineering and DIvERGE in *K. pneumoniae* ATCC 10031, we generated a novel version of pORTMAGE, termed pORTMAGE311B. This plasmid possesses a tightly regulated, XylS-Pm regulator/promoter-based λ Beta and *E. coli* MutL E32K co-expression system. On, pORTMAGE the expression of MutL E32K of *E. coli* abolishes methyl-directed mismatch repair (MMR) during the time-period of oligonucleotide incorporation into the bacterial genome(65). pORTMAGE311B ensured functionality at 37 °C and the rapid inducibility of λ Beta and E. coli MutL E32K by the addition of 1 mM m-Toluic-acid as an inducer. The temporal co-expression of λ Beta and MutL E32K also limits off-target mutagenic effects on the course of genome editing. Construction of pORTMAGE311B was performed by introducing the coding sequence of the dominant *E. coli mutL*(E32K) allele to the pSEVA258*beta* plasmid(66). To this aim, *mutL*(E32K) was PCR amplified from pORTMAGE2(65) using primers RBE32KF and XE32KR. The PCR product was then purified and digested with BamHI and XbaI. Next, the resulted fragment was cloned downstream of *beta* within pSEVA258*beta*. Finally, the successful assembly of the plasmid was verified by PCR and confirmed by capillary sequencing. pORTMAGE311B was also deposited to Addgene (Addgene Number 120418).

DIvERGE in *Klebsiella pneumoniae*

DIvERGE in *Klebsiella pneumoniae* ATCC 10031 was carried out according to a previously described DIvERGE workflow(21), with minor modifications. Briefly, *K. pneuomoniae* cells carrying pORTMAGE311B plasmid were inoculated into 2 ml LB medium + 50 µg/ml kanamycin and were grown at 37 °C, 250 rpm overnight. From this starter culture, 500 µl stationary phase culture was inoculated into 50 ml LB medium + 50 µg/ml kanamycin, and grown at 37 °C under continuous shaking at 250 rpm. Induction was initiated at OD_{600} = 0.4 by adding 50 µl 1 M m-Toluic-acid (Sigma-Aldrich, dissolved in 96% ethyl-alcohol). Induction was performed for 30 minutes at 37 °C. After induction, cells were cooled on ice for 15 minutes. Next, cells were washed 3-times with 50 ml sterile, ice-cold, ultra-pure distilled water. Finally, the cell pellet was resuspended in 800 µl sterile ultra-pure distilled water and kept on ice until electroporation.

To perform DIvERGE, and separately, the saturation mutagenesis of GyrA D82 and ParC D79, the corresponding *gyrA,* and *parC*-targeting oligos were equimolarly mixed at a final concentration of 500 µM and 2 µl of this oligo-mixture was added to 40 µl electrocompetent cell in 10 parallels. Following

the electroporation of each sample, the 10 parallel samples were pooled together, and immediately after electroporation cells were suspended in 50 ml TB to allow for cell recovery. After a 1-hour recovery period at 37 °C, 250 rpm, an additional 50 ml LB medium along with 50 µg/ml (final cc.) kanamycin was added. Next, cells were grown at 37 °C, 250 rpm for 24 hours. To select clones with reduced susceptibility to gepotidacin from this DIvERGE library, 500 µl cell library was spread to 6 µg/ml gepotidacin-containing MHBII agar plates and plates were incubated at 37 °C for 48 hours. Finally, 10 randomly selected colonies were analyzed by capillary sequencing (oligos: KPGA1F, KPGA1R and KPPC1F, KPPC1R) from both antibiotic-selected cell libraries.

Engineering mutations associated with reduced susceptibility to gepotidacin in *Escherichia coli*

To assess the phenotype of mutations associated with reduced susceptibility to gepotidacin, we individually reconstructed both GyrA D82N and ParC D79N mutations in *E. coli* K-12 MG1655. We utilized a previously described CRISPR-MAGE protocol to integrate mutations and counter select against the wild-type genotype(67, 68). Briefly, cell-containing pORTMAGE2 (Addgene #72677) were transformed with pCas9 (Addgene #42876) and were grown in LB + 100 µg/ml ampicillin + 20 µg/ml chloramphenicol broth at 30 ^{o}C. Next, pCRISPR plasmids (Addgene #42875) were constructed with crRNA sequences targeting the wild-type *gyrA* and *parC* loci in the vicinity of D82 and D79 according to a previously described protocol (oligos: ECGACRF1, ECGACRR1, and ECPCCRF1, ECPCCRR1, respectively). Following plasmid-construction, correct clones were identified by capillary sequencing. To integrate GyrA D82N and ParC D79N mutations into the chromosome of *E. coli*, induced pORTMAGE2 and pCas9-carrying cells were prepared and made electrocompetent. Next, simultaneously, 100 ng of the corresponding pCRISPR plasmid and 200 pmole of oligonucleotide (MGYRA82N or MPARC79N) per 40 µl electrocompetent cells were electroporated. Cell were allowed to recover in 1 ml TB media and grown in 5 ml LB + 100 µg/ml ampicillin + 20 µg/ml chloramphenicol broth at 30 °C overnight and then spread to LB + 50 µg/ml kanamycin + 20 µg/ml chloramphenicol agar plates. Finally, the presence of the correct mutations was identified by capillary sequencing of the oligo-targets (oligos: 25922Ga1, 25922Ga3, and 25922Pc1, 25922Pc3).

Engineering isogenic *Klebsiella* and *Salmonella* strains carrying mutations associated with reduced susceptibility to gepotidacin and fluoroquinolones

To investigate mutational effects on antibiotic susceptibility and growth phenotypes, mutations and mutation combinations linked to reduced susceptibility to gepotidacin and ciprofloxacin were reconstructed in *K. pneumoniae* ATCC 10031 and in *Salmonella enterica ssp. enterica* serovar *Typhimurium*. To this aim, specific point mutations (see Supplementary file 1) were inserted into the chromosome of *K. pneumoniae* by pORTMAGE-recombineering(21, 65). Briefly, pORTMAGE-recombineering was performed using pORTMAGE311B (Addgene #120418). 1 µl of 100 µM of the corresponding oligos or oligo-mixtures were used for ssDNA-recombineering in appropriate combinations to create mutations linked to reduced susceptibility to gepotidacin and ciprofloxacin. Following recombineering, cells were allowed to grow overnight in TB medium at 37°C, 250 rpm. Next, variants carrying ciprofloxacin resistance-conferring mutations were selected on LB + 100 ng/ml ciprofloxacin agar plates, while mutants carrying the GyrA D82N; ParC D79N mutation-combination were selected on MHBII + 6 µg/ml gepotidacin agar plates. Cells carrying individual mutations assocated with reduced susceptibility to gepotidacin were plated onto LB + 50 µg/ml kanamycin agar plates. To obtain individual colonies, cultures from each recombineering populations were diluted, and appropriate dilutions were spread to agar plates. Plates were incubated at 37 °C, and individual colonies were genotyped by allele-specific PCR (using oligos KPA82ASF, KPA82ASR, and KPC79ASF, KPC79ASR). Finally, positive clones were confirmed by capillary sequencing of the oligo-target region. The reconstruction of the clinically prevalent GyrA D82 mutation in combination with a ParC D79N mutation in *Salmonella enterica ssp. enterica* serovar *Typhimurium* LT2 were conducted similarly to the reconstruction of specific mutations in *K. pneumoniae*. Briefly, pORTMAGE311B-containing, induced *S. enterica* cells were made electrocompetent and transformed with 1 µl of SE_GA_D82N and SE_PC_D79N oligos that integrated the corresponding GyrA D82N and ParC D79N mutations into the bacterial chromosome. Next, mutants were selected on MHBII + 6 µg/ml gepotidacin agar plates at 37 °C. Finally, the presence of the two mutations was identified and validated by capillary sequencing using SEGAF1, SEGAR1, and SEPCF1, SEPCR1 oligos.

Adaptive laboratory evolution of ciprofloxacin resistance

Adaptive laboratory evolution experiments followed an established protocol for automated laboratory evolution(69) and aimed to maximize the drug-resistance increment during a fixed time period. At each transfer step, 10^7 bacterial cells were transferred to a new culture and adaptation were performed by passaging 6 independent populations of *Klebsiella pneumoniae* ATCC 10031 wild-type, *Escherichia coli* K-12 MG1655 wild-type, and *Escherichia coli* K-12 MG1655 Δ*mutS* in the presence of increasing ciprofloxacin concentrations. Experiments were conducted in 96-well plates, in MHBII medium, by utilizing a checker board layout to minimize and to monitor cross-contamination. These 96-well deep-well plates (0.5 ml, polypropylene, V-bottom) were covered with sandwich covers (Enzyscreen BV) to ensure an optimal oxygen exchange rate and limit evaporation and were shaken at 150 rpm at 37 ˚C. Twenty µl of each evolving culture was parallelly transferred into four independent wells containing 350 µl fresh medium and an increasing concentration of gepotidacin and ciprofloxacin (i.e., 0.5×, 1×, 1.5×, and 2.5× the concentration of the previous concentration step). Following cell transfer, each culture was allowed to grow for 48 h. At each transfer, cell growth was monitored by measuring the optical density at 600 nm (OD_{600}) (Biotek Synergy 2). Only populations with (i) vigorous growth (i.e., OD_{600} > 0.25) and (ii) the highest drug concentration were selected for further evolution. Accordingly, only one of the four populations was retained for each independently evolving strain. This protocol was designed to avoid population extinction and to ensure that populations with the highest level of resistance were propagated further during evolution. Samples from each transfer were frozen in 15% dimethyl-sulfoxide (DMSO) at −80 ˚C for further analysis. Adaptation of an individual population was terminated when the antibiotic concentration in the given well would have exceeded 200 µg/ml after the transfer. Cells from these, highly-drug resistant populations were frozen after the addition of 15% dimethyl-sulfoxide (DMSO) and were kept at −80 ˚C. Following adaptation, cells from each final population were spread onto MHBII agar plates and individual colonies were isolated.

Whole genome sequencing of adapted lines

Following adaptive laboratory evolution of ciprofloxacin resistance in *K. pneuomoniae* ATCC 10031 and *E. coli* K-12 MG1655, single colonies from three adapted lines were subjected to whole genome sequencing on Illumina HiSeq 4000. Prior to sequencing, gDNA was isolated from each adapted line and the corresponding wild-type strain by using GeneElute (Sigma Aldrich) gDNA isolation kit

according to the manufacturer's instructions. To perform DNA sequencing, sequencing libraries were constructed from the gDNAs by fragmenting samples to a mean fragment length of 300 bp. Next, sequencing libraries were prepared by using a TruSeq DNA PCR-Free Library Prep Kit (Illumina). Finally, sequencing libraries were sequenced on a single sequencing lane of Illumina HiSeq 4000 using a HiSeq 3000/4000 SBS Kit (300 cycles, FC-410-1003, Illumina) to generate 2 × 150 bp paired-end reads. Following sequencing, in order to determine the variants and to annotate the mutations, we mapped sequencing reads to their corresponding reference genomes with the mem subcommand of bwa 0.7.12-r1039 (Burrows-Wheeler Aligner(70)). The SNPs and INDELs were called with VarScan(71) v2.3.9 with the following parameters: min-reads2=4, min-coverage=30, min-var-freq=0.1, min-freq-for-hom=0.6, min-avg-qual=20, strand-filter=0. Only variants with prevalence higher than 60% were voted as mutations. Following variant calling, mutations were also manually inspected within the aligned reads, and adapted lines that become hypermutators (i.e. that are accumulated more than 55 mutations in a single lineage) were excluded from further analysis. Finally, the annotation of each mutation with genomic features was performed with the intersect subcommand of bedtools v2.25.0.

In vitro growth-rate measurements

We measured the growth phenotype of bacterial variants by assessing their growth at 37℃ in MHBII medium. To measure growth, we inoculated 5×10^4 cells from early stationary phase cultures (prepared in MHBII medium) into 100 µl of MHBII medium in a 96 well microtiter plate and monitored growth for 24 h. Bacterial growth was measure as the 600 nm optical density (OD_{600}) of cultures at a given timepoint. OD_{600} measurements were carried out every 5 minutes using BioTek Synergy 2 microplate reader while bacterial cultures were grown at 37℃ under continuous, variable intensity shaking. Each bacterial variant and their corresponding wild-types were measured in two consecutive experiments, with 12 replicates in each subsequent tests (24 biological replicates in total). Finally, growth rates were calculated from the obtained growth curves according to a previously described procedure(72, 73).

Competition-based fitness measurements

Competition assay-based fitness measurements were carried out by competing mutant strains against their corresponding wild-type strain carrying a *lacZ* knockout mutation. The *lacZ* knockout strain was constructed by integrating a premature stop codon in place the 23rd amino acid of LacZ with a previously reported pORTMAGE protocol(65). Briefly, heat-induced pORTMAGE3 (Addgene #72678) containing *K. pneuomoniae* ATCC 10031 cells were electroporated with KpLacZW23* oligonucleotide (2.5 nM final concentration). Following oligo-integration into the bacterial chromosome, *lacZ*(-) variants were identified by plating cells out to X-gal + IPTG-containing MHBII agar plates at appropriate dilution to form single colonies, where knockout mutants formed white colonies and could be easily distinguished from the dark blue colonies of the wild-type containing a functional β-galactosidase gene. Each competition experiment started by inoculating early stationary phase cultures in a 99:1, as mutant to wild-type ratio, into 10 ml MHBII medium at 1:1000-fold dilution and incubating each culture at 37 °C for 24 h under a constant agitation of 250 rpm. These cultures were then serially transferred into 10 ml fresh MHBII medium in a 1:1000 dilution in every 24 hours for 3 subsequent transfers. To analyze the composition of each population, cultures were plated onto X-gal + IPTG supplemented MHBII agar plates (in 145×20 mm Petri dishes, Greiner Bio-One Ltd) at appropriate dilutions to obtain approximately 1000 colonies per each plate. Plates were then incubated at 37 °C overnight. The ratio of the mutant (*lacZ* proficient, blue) and the wild-type (*lacZ* deficient, white) at each given time point was determined from the number of blue and white colonies on X-Gal + IPTG agar plates. Importantly, prior experiments showed that *lacZ* deficient K. pneumoniae cells suffer no competitive disadvantage compared to their corresponding wild-type strain. Competition experiments were performed in five replicates. Finally, selection coefficients were estimated as the slope of the change in ratio, as defined in the following equation:

$$\ln[x1(t)/x2(t)] = \ln[x1(0)/x2(0)] + st$$

where s is the selection coefficient, t is time or number of generations, x1 and x2 are the ratio of the two strains at a given time point(74).

Prevalence of mutations associated with reduced susceptibility to gepotidacin in sequence databases

In order to investigate if genotypes GyrA D82 and ParC D79N exist in bacteria, we downloaded all DNA sequences from NCBI nucleotide database (ftp://ftp.ncbi.nlm.nih.gov/blast/db/nt.??.tar.gz) using

wget 1.17.1 on 9 Oct 2018. We performed the BLAST search with tBLASTn 2.231(75) (build Jan 7 2016) on the downloaded full nucleotide database as subject and GyrA and ParC as query. Protein sequences of GyrA (P0AES4) and ParC (P0AFI2) were downloaded from UniProt. To perform BLAST, the database was fragmented and the BLAST search was carried out on these smaller datasets (with argument max_target_seqs = 20000). Finally, separately obtained results were merged. Finally, for each sequence the taxonomy of the source bacteria was assigned with blastdbcmd (version 2.2.31).

Mouse thigh infection models

Drug-resistant *K. pneumoniae* is frequently responsible for wound and systemic infections, therefore, we benchmarked *in vivo* effects of reduced susceptibility gepotidacin in a murine thigh wound infection model(29, 30). Specifically, we examined wound colonization for representative gepotidacin and ciprofloxacin-resistant mutants of *K. pneumoniae* ATCC 10031 and compared to that of the wild-type. Murine thigh infections were performed according to a previously established protocol(30, 76). Bacterial inoculums were prepared by inoculating single bacterial colonies into 5 ml of MHBII broth and were incubated at 37 °C for 16 hours under constant agitation (250 rpm). Next, ½ volume of 50 volume/volume% glycerol:water mixture was added to each culture and 550 µl of these cell suspensions were frozen at -80 °C. Before inoculation, cell suspensions were allowed to thaw at room temperature for 15 minutes. As test animals, groups of 5 female specific-pathogen-free ICR (CD-1) mice weighing 22 ± 2 g were used. Animals were immunosuppressed by two intraperitoneal injections of cyclophosphamide, the first at 150 mg/kg 4 days before infection (day –4) and the second at 100 mg/kg 1 day before infection (day –1). On day 0, animals were inoculated intramuscularly into the right thigh with 10^6 CFU/mouse of the corresponding pathogenic mutant (0.1 ml culture/thigh). After 26 hours inoculation, animals were humanely euthanized with CO_2 asphyxiation and then the muscle of the right thigh was harvested from each test animal. The removed muscle was homogenized in 3 ml of phosphate-buffered saline, pH 7.4, with a polytron homogenizer. Finally, 0.1 mls of these homogenates were used for serial 10-fold dilutions and plated onto LB agar for colony count (CFU/g) determination.

All aspects of this work including housing, experimentation, and animal disposal were performed in general accordance with the Guide for the Care and Use of laboratory animals (National

Academy Press, Washington, DC, 2011). All experiments were performed under ABSL2 conditions in the AAALAC(American Association for Accreditation of Laboratory Animal Care)-accredited vivarium of Eurofins Pharmacology Discovery Services Taiwan, Ltd. with the oversight of veterinarians to assure compliance with IACUC regulations and the humane treatment of laboratory animals.

Minimum Inhibitory Concentration measurements

Minimum Inhibitory Concentrations (MICs) were determined using a standard serial broth microdilution technique according to the EUCAST guidelines(77) (ISO 20776-1:2006, Part 1). Briefly, bacterial strains were inoculated from frozen cultures onto MHBII agar plates and were grown overnight at 37 °C. Next, independent colonies from each strain were inoculated into 1 ml MHBII medium and were propagated at 37 °C, 250 rpm overnight. To perform MIC assays, 12-step serial dilutions using 2-fold dilution-steps of the given antibiotic were generated in 96-well microtiter plates (Sarstedt 96-well microtest plate with lid, flat base). Antibiotics were diluted in 100 µl of MHBII medium. Following dilutions, each well was seeded with an inoculum of 5×10^4 bacterial cells. Each measurements were performed at least in 3 parallel replicates. Also, to avoid possible edge effects at the edge of the microwell plate, side-rows (A and H) contained only medium without bacterial cells. Following inoculations, plates were covered with lids and wrapped in polyethylene plastic bags to minimize evaporation but allow for aerobic O_2 transfer. Plates were incubated at 37 °C under continuous shaking at 150 rpm for 18 hours in an INFORS HT shaker. After incubation, OD_{600} of each well on the microwell plate was measured using a Biotek Synergy 2 microplate reader. MIC was defined as the antibiotic concentration which inhibited the growth of the bacterial culture, i.e., the drug concentration where the average OD_{600} increment of the three replicates was below 0.05.

Acknowledgments

We wish to thank Lynn Miesel, Andrea Tóth, Lucy Chia, and Tamás Kukli for their support. This work was supported by grants from the European Research Council H2020-ERC-2014-CoG 648364 'Resistance Evolution' (to C.P.), the Wellcome Trust (to C.P.), and GINOP (MolMedEx TUMORDNS) GINOP-2.3.2-15-2016-00020, GINOP (EVOMER) GINOP-2.3.2-15-2016-00014 (to C.P.), EFOP 3.6.3-VEKOP-16-2017-00009 (to P. Sz. and T.R.) and UNKP-18-3 New National Excellence Program of the Ministry of Human Capacities (to P. Sz.); the 'Lendület' Program of the Hungarian Academy of Sciences (to C.P.), an NKFIH grant K120220 (to B.K.), and a PhD fellowship from the Boehringer Ingelheim Fonds (to Á.N.). B.K. was supported by the UNKP-18-4 New National Excellence Program of the Ministry of Human Capacities, the János Bolyai Research Scholarship of the Hungarian Academy of Sciences, and M.C. was supported by the Szeged Scientists Academy under the sponsorship of the Hungarian Ministry of Human Capacities (EMMI: 13725-2/2018/INTFIN). The authors thank Dora Bokor PharmD for proofreading the manuscript and acknowledge KIFÜ for awarding us access to resource based in Hungary at Debrecen.

Authors' contributions

The research was conceived and supervised by Á.N., and C.P.; T.R., Á.N., G.D., P.S., F.B., and C.P. designed the experiments and interpreted experimental data. G.D., P.S., Á.N., G.F., M.S., T.R., D.B., L.D., R.S., T.M., M. C., G.G., B.K., V.B.M. performed the experiments or calculations.

Competing financial interests

The authors declare competing financial interest. Á.N., B.K., and C.P. have filed a patent application (PCT/EP2017/082574) related to DIvERGE.

References

1. Spellberg B, Powers JH, Brass EP, Miller LG, Edwards JE. 2004. Trends in Antimicrobial Drug Development: Implications for the Future. Clin Infect Dis 38:1279–1286.

2. Jackson, N., Czaplewski, L., & Piddock, L. J. (2018). Discovery and development of new antibacterial drugs: learning from experience?. Journal of Antimicrobial Chemotherapy, 73(6), 1452-1459.

3. Suzuki, S., Horinouchi, T., & Furusawa, C. (2015). Suppression of antibiotic resistance acquisition by combined use of antibiotics. Journal of bioscience and bioengineering, 120(4), 467-469.

4. Munck C, Gumpert HK, Wallin AIN, Wang HH, Sommer MOA. 2014. Prediction of resistance development against drug combinations by collateral responses to component drugs. Sci Transl Med 6:262ra156-262ra156.

5. Silver LL. 2007. Multi-targeting by monotherapeutic antibacterials. Nat Rev Drug Discov 6:41–55.

6. Klahn, P., & Brönstrup, M. (2017). Bifunctional antimicrobial conjugates and hybrid antimicrobials. Natural product reports, 34(7), 832-885.

7. Eliopoulos GM, Meka VG, Gold HS. 2004. Antimicrobial Resistance to Linezolid. Clin Infect Dis 39:1010–1015.

8. Farrell DJ, Sader HS, Rhomberg PR, Scangarella-Oman NE, Flamm RK. 2017. In Vitro Activity of Gepotidacin (GSK2140944) against Neisseria gonorrhoeae. Antimicrob Agents Chemother 61:e02047-16.

637 9. Dougherty TJ, Nayar A, Newman JV, Hopkins S, Stone GG, Johnstone M, Shapiro AB, Cronin M,
638 Reck F, Ehmann DE. 2014. NBTI 5463 Is a Novel Bacterial Type II Topoisomerase Inhibitor with
639 Activity against Gram-Negative Bacteria and In Vivo Efficacy. Antimicrob Agents Chemother
640 58:2657–2664.

641 10. Tari LW, Li X, Trzoss M, Bensen DC, Chen Z, Lam T, Zhang J, Lee SJ, Hough G, Phillipson D, Akers-
642 Rodriguez S, Cunningham ML, Kwan BP, Nelson KJ, Castellano A, Locke JB, Brown-Driver V,
643 Murphy TM, Ong VS, Pillar CM, Shinabarger DL, Nix J, Lightstone FC, Wong SE, Nguyen TB,
644 Shaw KJ, Finn J. 2013. Tricyclic GyrB/ParE (TriBE) inhibitors: a new class of broad-spectrum
645 dual-targeting antibacterial agents. PLoS ONE 8:e84409.

646 11. Wang KK, Stone LK, Lieberman TD, Shavit M, Baasov T, Kishony R. 2016. A Hybrid Drug Limits
647 Resistance by Evading the Action of the Multiple Antibiotic Resistance Pathway. Mol Biol Evol
648 33:492–500.

649 12. Pokrovskaya V, Belakhov V, Hainrichson M, Yaron S, Baasov T. 2009. Design, Synthesis, and
650 Evaluation of Novel Fluoroquinolone–Aminoglycoside Hybrid Antibiotics. J Med Chem
651 52:2243–2254.

652 13. Nayar AS, Dougherty TJ, Reck F, Thresher J, Gao N, Shapiro AB, Ehmann DE. 2015. Target-Based
653 Resistance in Pseudomonas aeruginosa and Escherichia coli to NBTI 5463, a Novel Bacterial
654 Type II Topoisomerase Inhibitor. Antimicrobial Agents and Chemotherapy 59:331–337.

655 14. Taylor, S. N., Morris, D. H., Avery, A. K., Workowski, K. A., Batteiger, B. E., Tiffany, C. A., ... &
656 Dumont, E. F. (2018). Gepotidacin for the treatment of uncomplicated urogenital gonorrhea: a
657 phase 2, randomized, dose-ranging, single-oral dose evaluation. Clinical Infectious Diseases,
658 67(4), 504-512.

15. O'Riordan W, Tiffany C, Scangarella-Oman N, Perry C, Hossain M, Ashton T, Dumont E. 2017. The Efficacy, Safety, and Tolerability of Gepotidacin (GSK2140944) in the Treatment of Patients with Suspected or Confirmed Gram-Positive Acute Bacterial Skin and Skin Structure Infections. Antimicrobial Agents and Chemotherapy AAC.02095-16.

16. Biedenbach DJ, Bouchillon SK, Hackel M, Miller LA, Scangarella-Oman NE, Jakielaszek C, Sahm DF. 2016. In Vitro Activity of Gepotidacin, a Novel Triazaacenaphthylene Bacterial Topoisomerase Inhibitor, against a Broad Spectrum of Bacterial Pathogens. Antimicrob Agents Chemother 60:1918–1923.

17. Flamm RK, Farrell DJ, Rhomberg PR, Scangarella-Oman NE, Sader HS. 2017. Gepotidacin (GSK2140944) In Vitro Activity against Gram-positive and Gram-negative Bacteria (MBC/MIC, Kill Kinetics, Checkerboard, PAE/SME tests). Antimicrob Agents Chemother AAC.00468-17.

18. Nyerges Á, Csörgő B, Draskovits G, Kintses B, Szili P, Ferenc G, Révész T, Ari E, Nagy I, Bálint B, Vásárhelyi BM, Bihari P, Számel M, Balogh D, Papp H, Kalapis D, Papp B, Pál C. 2018. Directed evolution of multiple genomic loci allows the prediction of antibiotic resistance. PNAS 201801646.

19. Tillotson, G. (2018). A crucial list of pathogens. The Lancet Infectious Diseases, 18(3), 234-236.

20. Kollman PA, Massova I, Reyes C, Kuhn B, Huo S, Chong L, Lee M, Lee T, Duan Y, Wang W, Donini O, Cieplak P, Srinivasan J, Case DA, Cheatham TE. 2000. Calculating Structures and Free Energies of Complex Molecules: Combining Molecular Mechanics and Continuum Models. Acc Chem Res 33:889–897.

21. Nyerges Á, Csörgő B, Draskovits G, Kintses B, Szili P, Ferenc G, Révész T, Ari E, Nagy I, Bálint B, Vásárhelyi BM, Bihari P, Számel M, Balogh D, Papp H, Kalapis D, Papp B, Pál C. 2018. Directed

evolution of multiple genomic loci allows the prediction of antibiotic resistance. PNAS 115:E5726–E5735.

22. Hughes D, Andersson DI. 2015. Evolutionary consequences of drug resistance: shared principles across diverse targets and organisms. Nat Rev Genet 16:459–471.

23. Martínez JL, Baquero F, Andersson DI. 2011. Beyond serial passages: new methods for predicting the emergence of resistance to novel antibiotics. Current Opinion in Pharmacology 11:439–445.

24. Sommer, M. O., Munck, C., Toft-Kehler, R. V., & Andersson, D. I. (2017). Prediction of antibiotic resistance: time for a new preclinical paradigm?. Nature Reviews Microbiology, 15(11), 689.

25. Andersson DI. 2015. Improving predictions of the risk of resistance development against new and old antibiotics. Clinical Microbiology and Infection 21:894–898.

26. Krapp, F., Ozer, E. A., Qi, C., & Hauser, A. R. (2018, April). Case report of an extensively drug-resistant Klebsiella pneumoniae infection with genomic characterization of the strain and review of similar cases in the United States. In Open forum infectious diseases (Vol. 5, No. 5, p. ofy074). US: Oxford University Press..

27. Weigel LM, Steward CD, Tenover FC. 1998. gyrA Mutations Associated with Fluoroquinolone Resistance in Eight Species ofEnterobacteriaceae. Antimicrob Agents Chemother 42:2661–2667.

28. Chen F-J, Lauderdale T-L, Ho M, Lo H-J. 2003. The Roles of Mutations in *gyrA, parC* , and *ompK35* in Fluoroquinolone Resistance in *Klebsiella pneumoniae*. Microbial Drug Resistance 9:265–271.

29. Velkov, T., Bergen, P. J., Lora-Tamayo, J., Landersdorfer, C. B., & Li, J. (2013). PK/PD models in antibacterial development. Current opinion in microbiology, 16(5), 573-579.

30. Tan CM, Therien AG, Lu J, Lee SH, Caron A, Gill CJ, Lebeau-Jacob C, Benton-Perdomo L, Monteiro JM, Pereira PM, Elsen NL, Wu J, Deschamps K, Petcu M, Wong S, Daigneault E, Kramer S, Liang L, Maxwell E, Claveau D, Vaillancourt J, Skorey K, Tam J, Wang H, Meredith TC, Sillaots S, Wang-Jarantow L, Ramtohul Y, Langlois E, Landry F, Reid JC, Parthasarathy G, Sharma S, Baryshnikova A, Lumb KJ, Pinho MG, Soisson SM, Roemer T. 2012. Restoring Methicillin-Resistant Staphylococcus aureus Susceptibility to β-Lactam Antibiotics. Science Translational Medicine 4:126ra35-126ra35.

31. Hooper DC, Jacoby GA. 2016. Topoisomerase Inhibitors: Fluoroquinolone Mechanisms of Action and Resistance. Cold Spring Harb Perspect Med 6:a025320.

32. Gibson EG, Ashley RE, Kerns RJ, Osheroff N. 2018. Bacterial Type II Topoisomerases and Target-Mediated Drug Resistance, p. 507–529. *In* Fong, IW, Shlaes, D, Drlica, K (eds.), Antimicrobial Resistance in the 21st Century. Springer International Publishing, Cham.

33. Wohlkonig A, Chan PF, Fosberry AP, Homes P, Huang J, Kranz M, Leydon VR, Miles TJ, Pearson ND, Perera RL, Shillings AJ, Gwynn MN, Bax BD. 2010. Structural basis of quinolone inhibition of type IIA topoisomerases and target-mediated resistance. Nat Struct Mol Biol 17:1152–1153.

34. Collin F, Karkare S, Maxwell A. 2011. Exploiting bacterial DNA gyrase as a drug target: current state and perspectives. Appl Microbiol Biotechnol 92:479–497.

35. Correia S, Poeta P, Hébraud M, Capelo JL, Igrejas G. 2017. Mechanisms of quinolone action and resistance: where do we stand? Journal of Medical Microbiology 66:551–559.

36. Scangarella-Oman NE, Hossain M, Dixon PB, Ingraham K, Min S, Tiffany CA, Perry CR, Raychaudhuri A, Dumont EF, Huang J, Hook EW, Miller LA. 2018. Microbiological Analysis From

a Phase 2 Randomized Study in Adults Evaluating Single Oral Doses of Gepotidacin in the Treatment of Uncomplicated Urogenital Gonorrhea Caused by Neisseria gonorrhoeae. Antimicrobial Agents and Chemotherapy AAC.01221-18.

37. Bell, G., & MacLean, C. (2018). The search for 'evolution-proof'antibiotics. Trends in Microbiology, 26(6), 471-483.

38. Martínez JL, Baquero F, Andersson DI. 2007. Predicting antibiotic resistance. Nat Rev Micro 5:958–965.

39. Lázár V, Martins A, Spohn R, Daruka L, Grézal G, Fekete G, Számel M, Jangir PK, Kintses B, Csörgo B, Nyerges Á, Györkei Á, Kincses A, Dér A, Walter FR, Deli MA, Urbán E, Hegedus Z, Olajos G, Méhi O, Bálint B, Nagy I, Martinek T, Papp B, Pál C. 2018. Antibiotic-resistant bacteria show widespread collateral sensitivity to antimicrobial peptides. Nature microbiology 3:718–731.

40. Baym M, Lieberman TD, Kelsic ED, Chait R, Gross R, Yelin I, Kishony R. 2016. Spatiotemporal microbial evolution on antibiotic landscapes. Science 353:1147–1151.

41. The European Committee on Antimicrobial Susceptibility Testing E 2018. EUCAST: Clinical breakpoints. EUCAST: Clinical breakpoints, The European Committee on Antimicrobial Susceptibility Testing. (http://www.eucast.org/clinical_breakpoints/)

42. Miles TJ, Hennessy AJ, Bax B, Brooks G, Brown BS, Brown P, Cailleau N, Chen D, Dabbs S, Davies DT, Esken JM, Giordano I, Hoover JL, Jones GE, Kusalakumari Sukmar SK, Markwell RE, Minthorn EA, Rittenhouse S, Gwynn MN, Pearson ND. 2016. Novel tricyclics (e.g., GSK945237) as potent inhibitors of bacterial type IIA topoisomerases. Bioorganic & Medicinal Chemistry Letters 26:2464–2469.

747 43. Harkins, C. P., Pichon, B., Doumith, M., Parkhill, J., Westh, H., Tomasz, A., ... & Holden, M. T.
748 (2017). Methicillin-resistant Staphylococcus aureus emerged long before the introduction of
749 methicillin into clinical practice. Genome biology, 18(1), 130.

750 44. Marcusson LL, Frimodt-Møller N, Hughes D. 2009. Interplay in the Selection of Fluoroquinolone
751 Resistance and Bacterial Fitness. PLOS Pathogens 5:e1000541.

752 45. Hooper DC, Jacoby GA. 2015. Mechanisms of drug resistance: quinolone resistance. Ann N Y
753 Acad Sci 1354:12–31.

754 46. Weinstein ZB, Zaman MH. 2018. Evolution of rifampicin resistance due to substandard drugs in
755 E. coli and M. smegmatis. Antimicrobial Agents and Chemotherapy AAC.01243-18.

756 47. Boeckel TPV, Gandra S, Ashok A, Caudron Q, Grenfell BT, Levin SA, Laxminarayan R. 2014.
757 Global antibiotic consumption 2000 to 2010: an analysis of national pharmaceutical sales data.
758 The Lancet Infectious Diseases 14:742–750.

759 48. Taylor SN, Marrazzo J, Batteiger BE, Hook EW, Seña AC, Long J, Wierzbicki MR, Kwak H,
760 Johnson SM, Lawrence K, Mueller J. 2018. Single-Dose Zoliflodacin (ETX0914) for Treatment of
761 Urogenital Gonorrhea. New England Journal of Medicine 379:1835–1845.

762 49. Basarab GS, Kern GH, McNulty J, Mueller JP, Lawrence K, Vishwanathan K, Alm RA, Barvian K,
763 Doig P, Galullo V, Gardner H, Gowravaram M, Huband M, Kimzey A, Morningstar M, Kutschke
764 A, Lahiri SD, Perros M, Singh R, Schuck VJA, Tommasi R, Walkup G, Newman JV. 2015.
765 Responding to the challenge of untreatable gonorrhea: ETX0914, a first-in-class agent with a
766 distinct mechanism-of-action against bacterial Type II topoisomerases. Scientific Reports
767 5:11827.

768 50. Foerster, S., Golparian, D., Jacobsson, S., Hathaway, L. J., Low, N., Shafer, W. M., ... & Unemo,
769 M. (2015). Genetic resistance determinants, in vitro time-kill curve analysis and

770 pharmacodynamic functions for the novel topoisomerase II inhibitor ETX0914 (AZD0914) in
771 Neisseria gonorrhoeae. Frontiers in microbiology, 6, 1377.

772 51. Damião Gouveia AC, Unemo M, Jensen JS. 2018. In vitro activity of zoliflodacin (ETX0914)
773 against macrolide-resistant, fluoroquinolone-resistant and antimicrobial-susceptible
774 Mycoplasma genitalium strains. J Antimicrob Chemother 73:1291–1294.

775 52. The Pew Charitable Trusts. Antibiotics Currently in Clinical Development.
776 (https://www.pewtrusts.org/en/research-and-analysis/data-visualizations/2014/antibiotics-
777 currently-in-clinical-development)

778 53. 2017. Small-Molecule Drug Discovery Suite 2017-4. Schrödinger, LLC, New York, NY.

779 54. 2016. Marvin 16.2.1. Chemaxon (http://www.chemaxon.com).

780 55. Harder E, Damm W, Maple J, Wu C, Reboul M, Xiang JY, Wang L, Lupyan D, Dahlgren MK,
781 Knight JL, Kaus JW, Cerutti DS, Krilov G, Jorgensen WL, Abel R, Friesner RA. 2016. OPLS3: A
782 Force Field Providing Broad Coverage of Drug-like Small Molecules and Proteins. Journal of
783 Chemical Theory and Computation 12:281–296.

784 56. Berendsen HJC, Postma JPM, van Gunsteren WF, Hermans J. 1981. Interaction Models for
785 Water in Relation to Protein Hydration, p. 331–342. *In* Pullman, B (ed.), Intermolecular Forces.
786 Springer Netherlands, Dordrecht.

787 57. Kevin J. Bowers EC Huafeng Xu, Ron O Dror, Michael P Eastwood, Brent A Gregersen, John L
788 Klepeis, Istvan Kolossvary, Mark A Moraes, Federico D Sacerdoti, John K Salmon, Yibing Shan,
789 and David E Shaw. 2006. Scalable Algorithms for Molecular Dynamics Simulations on
790 Commodity Clusters. ACM/IEEE, Tampa, Florida.

791 58. 2017. Schrödinger Release 2017-4: Bioluminate. Schrödinger, LLC, New York, NY.

792 59. Kollman PA, Massova I, Reyes C, Kuhn B, Huo S, Chong L, Lee M, Lee T, Duan Y, Wang W, Donini
793 O, Cieplak P, Srinivasan J, Case DA, Cheatham TE. 2000. Calculating Structures and Free
794 Energies of Complex Molecules: Combining Molecular Mechanics and Continuum Models. Acc
795 Chem Res 33:889–897.

796 60. Sirin S, Pearlman DA, Sherman W. 2014. Physics-based enzyme design: Predicting binding
797 affinity and catalytic activity. Proteins: Structure, Function, and Bioinformatics 82:3397–3409.

798 61. Chrencik JE, Roth CB, Terakado M, Kurata H, Omi R, Kihara Y, Warshaviak D, Nakade S, Asmar-
799 Rovira G, Mileni M, Mizuno H, Griffith MT, Rodgers C, Han GW, Velasquez J, Chun J, Stevens RC,
800 Hanson MA. 2015. Crystal Structure of Antagonist Bound Human Lysophosphatidic Acid
801 Receptor 1. Cell 161:1633–1643.

802 62. Krishnamurthy VR, Sardar MYR, Ying Y, Song X, Haller C, Dai E, Wang X, Hanjaya-Putra D, Sun L,
803 Morikis V, Simon SI, Woods RJ, Cummings RD, Chaikof EL. 2015. Glycopeptide analogues of
804 PSGL-1 inhibit P-selectin in vitro and in vivo. Nature Communications 6:6387.

805 63. Lyne PD, Lamb ML, Saeh JC. 2006. Accurate Prediction of the Relative Potencies of Members of
806 a Series of Kinase Inhibitors Using Molecular Docking and MM-GBSA Scoring. J Med Chem
807 49:4805–4808.

808 64. Greenidge PA, Kramer C, Mozziconacci J-C, Wolf RM. 2013. MM/GBSA Binding Energy
809 Prediction on the PDBbind Data Set: Successes, Failures, and Directions for Further
810 Improvement. J Chem Inf Model 53:201–209.

811 65. Nyerges, Á., Csörgő, B., Nagy, I., Bálint, B., Bihari, P., Lázár, V., ... & Pál, C. (2016). A highly
812 precise and portable genome engineering method allows comparison of mutational effects
813 across bacterial species. Proceedings of the National Academy of Sciences, 113(9), 2502-2507.

814 66. Ricaurte DE, Martínez-García E, Nyerges Á, Pál C, Lorenzo V de, Aparicio T. 2018. A
815 standardized workflow for surveying recombinases expands bacterial genome-editing
816 capabilities. Microbial Biotechnology 11:176–188.

817 67. Jiang W, Bikard D, Cox D, Zhang F, Marraffini LA. 2013. RNA-guided editing of bacterial
818 genomes using CRISPR-Cas systems. Nat Biotech 31:233–239.

819 68. Umenhoffer K, Draskovits G, Nyerges Á, Karcagi I, Bogos B, Tímár E, Csörgő B, Herczeg R, Nagy
820 I, Fehér T, Pál C, Pósfai G. 2017. Genome-Wide Abolishment of Mobile Genetic Elements Using
821 Genome Shuffling and CRISPR/Cas-Assisted MAGE Allows the Efficient Stabilization of a
822 Bacterial Chassis. ACS Synth Biol 6:1471–1483.

823 69. Bódi Z, Farkas Z, Nevozhay D, Kalapis D, Lázár V, Csörgő B, Nyerges Á, Szamecz B, Fekete G,
824 Papp B, Araújo H, Oliveira JL, Moura G, Santos MAS, Jr TS, Balázsi G, Pál C. 2017. Phenotypic
825 heterogeneity promotes adaptive evolution. PLOS Biology 15:e2000644.

826 70. Li H, Durbin R. 2009. Fast and accurate short read alignment with Burrows–Wheeler transform.
827 Bioinformatics 25:1754–1760.

828 71. Koboldt DC, Zhang Q, Larson DE, Shen D, McLellan MD, Lin L, Miller CA, Mardis ER, Ding L,
829 Wilson RK. 2012. VarScan 2: Somatic mutation and copy number alteration discovery in cancer
830 by exome sequencing. Genome Res 22:568–576.

831 72. Warringer J, Ericson E, Fernandez L, Nerman O, Blomberg A. 2003. High-resolution yeast
832 phenomics resolves different physiological features in the saline response. PNAS 100:15724–
833 15729.

834 73. Karcagi I, Draskovits G, Umenhoffer K, Fekete G, Kovács K, Méhi O, Balikó G, Szappanos B,
835 Györfy Z, Fehér T, Bogos B, Blattner FR, Pál C, Pósfai G, Papp B. 2016. Indispensability of

836 Horizontally Transferred Genes and Its Impact on Bacterial Genome Streamlining. Mol Biol Evol
837 33:1257–1269.

838 74. Dykhuizen DE. 1990. Experimental Studies of Natural Selection in Bacteria. Annual Review of
839 Ecology and Systematics 21:373–398.

840 75. Altschul SF, Gish W, Miller W, Myers EW, Lipman DJ. 1990. Basic local alignment search tool.
841 Journal of Molecular Biology 215:403–410.

842 76. DeRyke CA, Banevicius MA, Fan HW, Nicolau DP. 2007. Bactericidal Activities of Meropenem
843 and Ertapenem against Extended-Spectrum-β-Lactamase-Producing Escherichia coli and
844 Klebsiella pneumoniae in a Neutropenic Mouse Thigh Model. Antimicrobial Agents and
845 Chemotherapy 51:1481–1486.

846 77. ISO (International Organization for Standardization). (2006). ISO 20776-1: 2006 Clinical
847 laboratory testing and in vitro diagnostic test systems–Susceptibility testing of infectious
848 agents and evaluation of performance of antimicrobial susceptibility test devices–Part 1:
849 Reference method for testing the in vitro activity of antimicrobial agents against rapidly
850 growing aerobic bacteria involved in infectious diseases. International Organization for
851 Standardization.

852

853

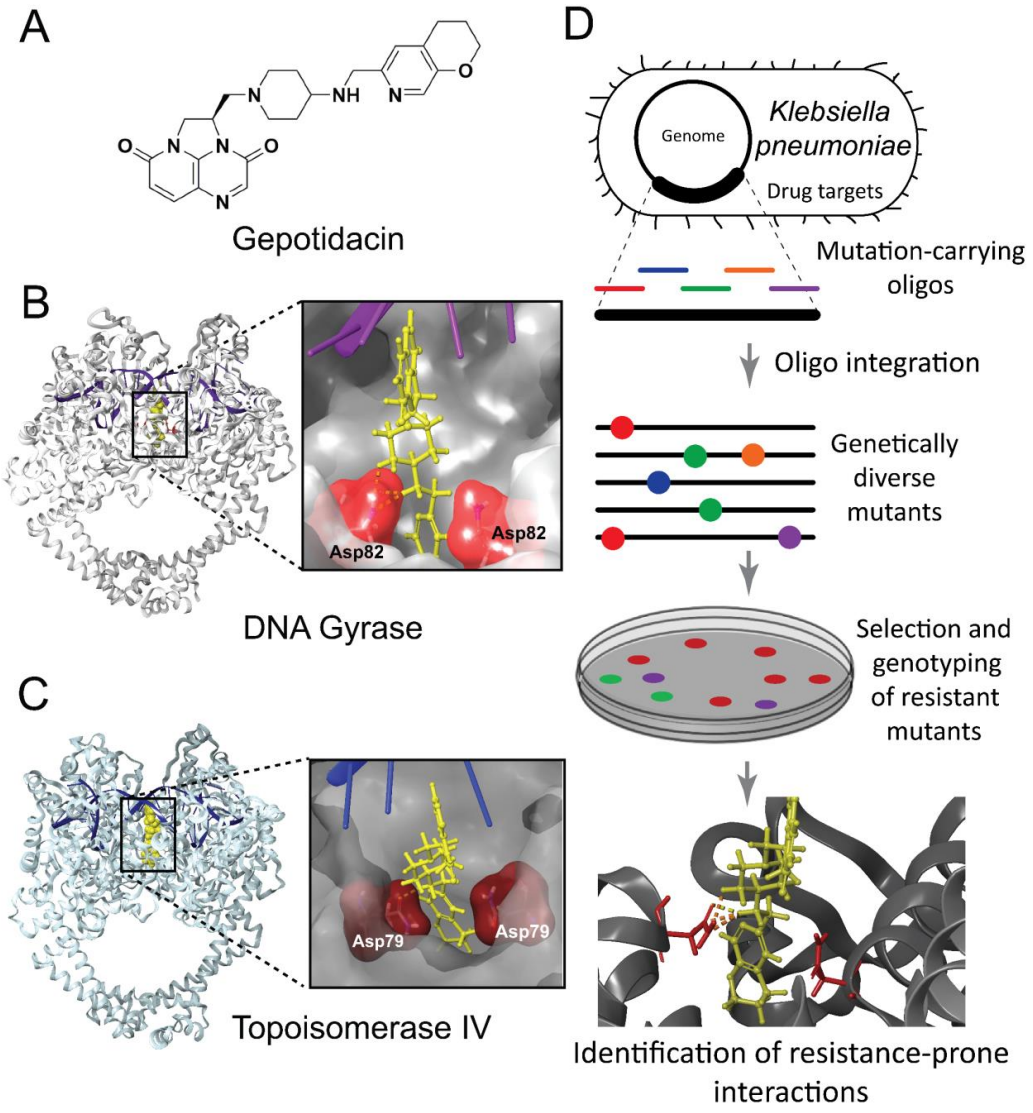

Figure 1. Binding site analysis of gepotidacin based on directed evolution and molecular modelling. (**A**) Gepotidacin, a novel triazaacenaphthylene antibiotic candidate inhibits DNA gyrase and topoisomerase IV in Gram-negative bacteria. (**B-C**) Ribbon representation of *E. coli*'s DNA gyrase- and topoisomerase IV in complex with gepotidacin, based on molecular dynamics simulations. Inlet shows the close-up view of gepotidacin (yellow) and its interacting residues (red) in a stick model. DNA is shown in magenta and blue. (**D**) The workflow of *in vivo* directed evolution of reduced susceptibility to gepotidacin in *K. pneumoniae* ATCC 10031.

	Gepotidacin MIC	**Ciprofloxacin MIC**

	(µg/ml)	(µg/ml)
***E. coli* K-12 MG1655 wild-type**	0.25	0.016
***E. coli* K-12 MG1655 GyrA D82N**	0.5	0.125
***E. coli* K-12 MG1655 ParC D79N**	0.5	0.016
***E. coli* K-12 MG1655 GyrA D82N; ParC D79N**	>256	0.25
***K. pneumoniae ssp. pneumoniae* ATCC 10031 wild-type**	0.063	0.004
***K. pneumoniae ssp. pneumoniae* ATCC 10031 GyrA D82N**	0.5	0.063
***K. pneumoniae ssp. pneumoniae* ATCC 10031 ParC D79N**	0.125	0.008
***K. pneumoniae ssp. pneumoniae* ATCC 10031 GyrA D82N; ParC D79N**	256	0.063

Table 1. Gepotidacin and ciprofloxacin minimal inhibitory concentration of single-step mutations and their combination in *Escherichia coli* K-12 MG1655 and *Klebsiella pneumoniae* ATCC 10031. Growth inhibition was determined by optical density (OD_{600}) measurements of the bacterial culture after 18 h incubation in the presence of the corresponding drug concentration, according to the EUCAST guidelines(77). Results presented here as the mean of 9 independent replicates respectively.

870 **(A)**

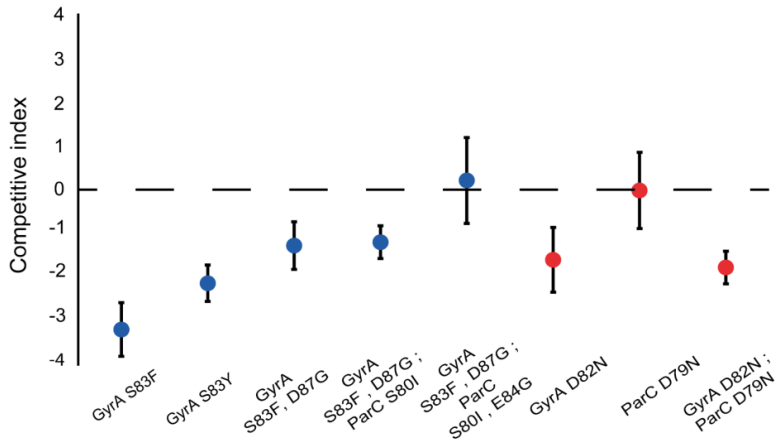

871

872 **(B)**

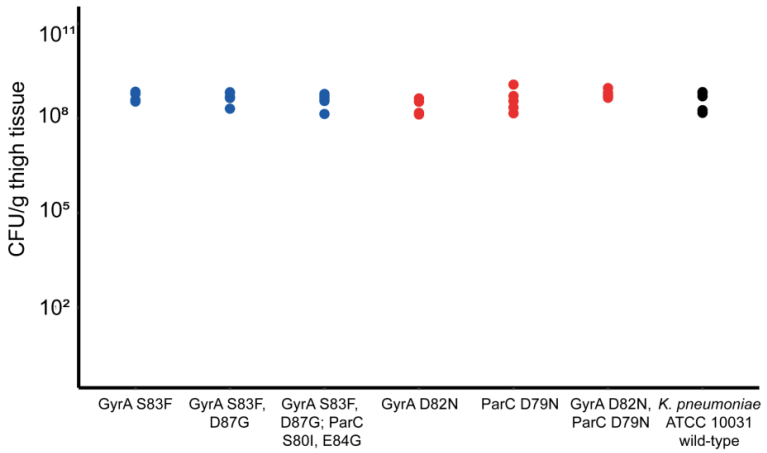

873

874

875 **Figure 2.** ***Fitness cost and virulence of bacteria with reduced susceptibility to gepotidacin*****. (A)**
876 In vitro competition between mutant and wild-type Klbsiella pneumoniae. Isogenic mutants of
877 *Klebsiella pneumoniae* ATCC 10031 carrying either a mutation combination conferring to reduced
878 susceptibility to gepotidacin or its single-step constituents (red), or clinically-occurring fluoroquinolone
879 resistance-associated mutations (blue) competed against the wild-type strain. In competition assays,
880 a competitive index <0 indicates that the wild-type population outcompetes the mutant population, and
881 conversely, a competition index >0 indicates that the mutant population outcompetes the wild-type
882 population. Error bars indicate standard deviation (SD) based on five biological replicates. **(B)**

Virulence of Klebsiella pneumoniae mutants and the wild-type strain in a murine thigh infection model. Bacterial burden in infected thigh tissues after 26 hours of infection caused by wild-type Klebsiella pneumoniae ATCC 10031 (black) or isogenic mutants carrying either mutations causing reduced susceptibility to gepotidacin or its single-step constituents (red), or clinically-occurring mutations associated with fluoroquinolone resistance (blue). The bacterial burden was assayed in Colony Forming Units (CFU)/g of tissue (n = 5 animals per data point, see Methods for details). No mutants were found to display a significant difference in virulence compared to the wild-type strain (t-test, $P > 0.05$ for all pairwise comparisons).

892 **(A)**

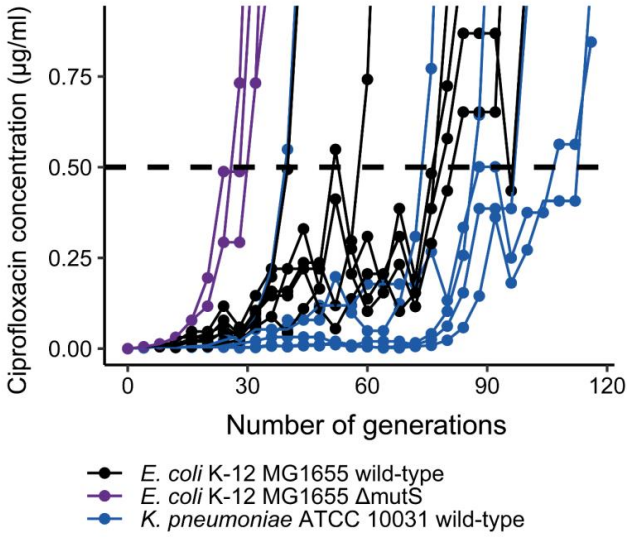

893

894 **(B)**

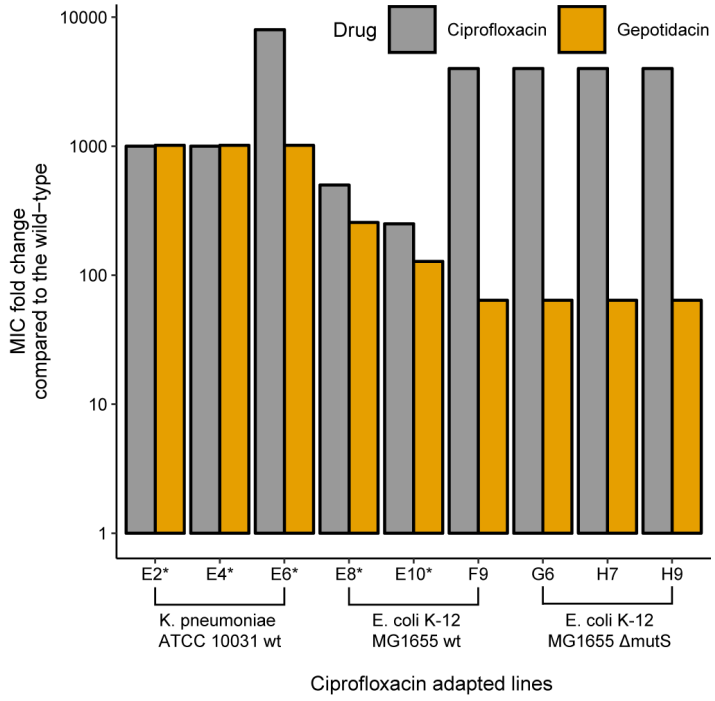

895

896

897 **Figure 3. Adaptive laboratory evolution of *Klebsiella pneumoniae* and *Escherichia coli* under**

898 **ciprofloxacin stress. (A)** Figure shows the antibiotic concentrations at which *K. pneumoniae* ATCC

10031, *as well as E. coli* K-12 MG1655 wild-type and Δ*mutS* hypermutator strains were able to grow under increasing ciprofloxacin stress as a function of time (number of cell generations). Dashed line represents the clinical breakpoint of ciprofloxacin resistance according to EUCAST(41). **(B)** Relative resistance level of the evolved lines against ciprofloxacin (grey bars) and gepotidacin (yellow bars) compared to the wild type at the end of the adaptive laboratory evolution. Asterisk (*) indicates that the evolved line was subjected to whole genome sequence analysis to uncover mutational processes behind the reduced susceptibility.